# Stabilization of Platinum Oxygen-Reduction Electrocatalysts Using Gold Clusters

J. Zhang,[1] K. Sasaki,[1] E. Sutter,[2] R. R. Adzic[1]

We demonstrated that platinum (Pt) oxygen-reduction fuel-cell electrocatalysts can be stabilized against dissolution under potential cycling regimes (a continuing problem in vehicle applications) by modifying Pt nanoparticles with gold (Au) clusters. This behavior was observed under the oxidizing conditions of the $O_2$ reduction reaction and potential cycling between 0.6 and 1.1 volts in over 30,000 cycles. There were insignificant changes in the activity and surface area of Au-modified Pt over the course of cycling, in contrast to sizable losses observed with the pure Pt catalyst under the same conditions. In situ x-ray absorption near-edge spectroscopy and voltammetry data suggest that the Au clusters confer stability by raising the Pt oxidation potential.

After Haruta's discovery (*1*) of the catalytic activity of supported small Au clusters for CO oxidation, there were several reports on the effects of the oxide supports in facilitating this activity (*1*–*3*). Other explanations of the activity included the clusters' distinct electronic (*4*) or chemical properties (*5*). The mechanism of oxygen adsorption and activation necessary for rapid CO oxidation is controversial and opposite to the observed lack of $O_2$ dissociation on Au single crystals (*6*). Recently, Chen and Goodman (*7*) suggested that all reactants adsorb on Au rather than on the oxide support. The metal oxide/support interface boundary sites are believed to be important for stabilizing oxygen-containing reaction intermediates on Au clusters (*8*). Support effects were reported on the nucleation, growth, and morphology of Au nanoclusters for $TiO_2$ and $SiO_2$ oxides (*9*).

As the underlying surface affects the Au clusters, so the clusters can conversely be expected to alter the properties of the support surfaces. However, such effects have not yet been studied, despite considerable scientific and technological interest. Here we report that Au clusters have a stabilizing effect on an underlying Pt metal surface under highly oxidizing conditions and suppress Pt dissolution during the $O_2$ reduction reaction (ORR) during potential cycling, without decreasing the oxygen reduction kinetics.

Fuel cells are expected to become a major source of clean energy (*10*, *11*) with particularly important applications in transportation. Despite considerable recent advances, existing fuel-cell technology still has drawbacks, including the instability of the Pt electrocatalyst for the ORR at the cathode (*10*). Recent work recorded a substantial loss of the Pt surface area over time in proton-exchange membrane fuel cells (PEMFCs) (*11*) during the stop-and-go driving of an electric car; this depletion exceeded the Pt dissolution rates observed upon holding at constant potentials (*12*) for extended time spans. Our results show promise toward resolving this impediment.

The Au clusters were deposited on a Pt catalyst (carbon-supported Pt nanoparticles) through galvanic displacement by Au of a Cu monolayer on Pt (*13*). Underpotential deposition, which involves a monolayer-limited process at potentials above the thermodynamic values, was used to coat a Pt surface with a monolayer of Cu. To obtain some insights into a possible mechanism of Au cluster formation on Pt nanoparticles, we describe a more tractable model system: depositing Au onto a single-crystal Pt(111) substrate. In addition, the Pt(111) surface is known to form a surface oxide layer that inhibits ORR activity and leads to its possible dissolution. It is likely that Au clusters can affect this process, which can provide information on the stabilization effect. After undergoing several potential sweeps to 1.2 V, the Au monolayer transformed into three-dimensional clusters (Fig. 1). The scanning tunneling microscopy (STM) image shows clusters two to three monolayers thick and 2 to 3 nm in diameter. All potentials are given with respect to a reversible hydrogen electrode (RHE). The measurements were carried out at room temperature, unless otherwise indicated.

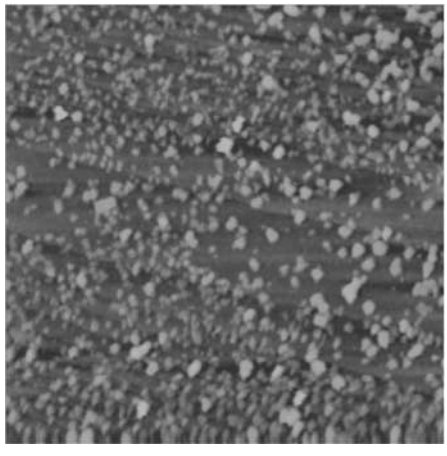

**Fig. 1.** STM image (125 × 125 nm) of the Au clusters on a Pt(111) surface, obtained by galvanic displacement of a Cu monolayer by Au. A Cu monolayer was deposited at underpotential on Pt (111). The Au adlayer was subjected to 10 cycles between 0.2 and 1.2 V versus RHE with a sweep rate of 50 mV/s to obtain such clusters. The STM image was acquired at the electrode potential of 0.8 V in 0.1 M $HClO_4$ at room temperature; the tunneling current was 1.24 nA.

The Au clusters on carbon-supported Pt nanoparticles were generated using the same method. Because the size of the Pt nanoparticles is about 3 nm, the Au clusters on Au/Pt/C are clearly much smaller than those on Au/Pt(111). We used the adsorption and oxidative desorption of CO to determine the Pt surface area blocked by Au. A thin layer of catalyst was bonded by a thin Nafion film to a glassy carbon disk of a rotating disk electrode. The CO stripping measurements on Pt/C and Au/Pt/C (fig. S1) revealed that the Au clusters in Au/Pt/C covered about 30 to 40% of the Pt surface. We assumed in this calculation that CO is not adsorbed on the Au surface under these conditions.

The structure of the Au-modified Pt/C catalyst was examined by high-resolution transmission electron microscopy. Measurements were performed using a high-resolution 300-kV field-

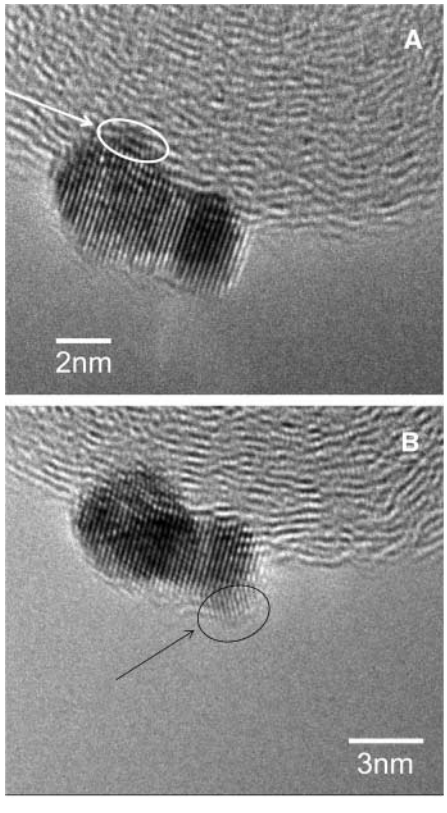


**Fig. 2.** Electron micrographs of a Au/Pt/C catalyst made by displacement of a Cu monolayer by Au. High-resolution images (**A** and **B**) show atomic rows with spacings that are consistent with the Pt(111) single-crystal structure. A different structure in the areas indicated by the arrows is ascribed to the Au clusters.

[1]Department of Chemistry, Brookhaven National Laboratory, Upton, NY 11973, USA. [2]Center for Functional Nanomaterials, Brookhaven National Laboratory, Upton, NY 11973, USA.

emission microscope (JEOL3000F) equipped with an energy filter, an energy-dispersive x-ray spectrometer, and an electron energy-loss spectrometer. Low-magnification images (fig. S2) indicate the presence of metal particles averaging 3 to 5 nm in size on ~50-nm carbon spheres. Figure 2 shows the morphology of two isolated metal nanoparticles on the carbon support. Energy-dispersive spectroscopy applied directly to these particles showed the presence of 10 to 11% Au on Pt. The most frequently observed lattice fringes fit well with the Pt(111) surface. The distinct structures indicated by arrows in Fig. 2 are ascribed to the Au clusters, which appear amorphous rather than crystalline.

The in situ extended x-ray absorption fine structure (EXAFS) spectra (fig. S3) of the Pt $L_3$ and Au $L_3$ edges of the Au/Pt/C electrocatalyst have an absorption intensity at the Au $L_3$ edge (11,919 eV) that is ~28% of that at the Pt $L_3$ edge (11,564 eV). The difference between the absorption intensities approximates the composition of the Au/Pt electrocatalyst because of the proximity of Pt and Au absorption coefficients. The mole ratio of bulk atoms to surface atoms for the 2- to 3-nm size of these nanoparticles is ~40 to 50%. If a 2/3 monolayer of Au is deposited on the surfaces of Pt nanoparticles, the Pt:Au mole ratio must thus range from 1:0.26 to 1:0.33, which is in a very good agreement with the above result of 28% (that is, 1:0.28) from EXAFS spectra. Because Au $L_3$ absorption begins only 355 eV after the onset of the Pt $L_3$ edge, some fluctuations due to photoelectron scattering in the Pt EXAFS spectrum must be superimposed on the Au spectrum. The proximity of the Pt and Au $L_3$ edges makes the analysis of such spectra questionable. Thus, the size of the Au clusters could not be determined.

We found that the Pt nanoparticles retain their ORR activity crucial for fuel-cell catalysts after the deposition of Au clusters. On a rotating disc-ring electrode, the activities of Au/Pt/C and Pt/C differed by only 3 mV, expressed as the half-wave potential of these two surfaces (fig. S4). The small difference in the ring currents of the two surfaces corroborates this conclusion. In addition, the ring currents show a negligible generation of $H_2O_2$, indicating a four-electron reduction of $O_2$ to $H_2O$ on both surfaces.

The stabilizing effect of Au clusters on Pt was determined in an accelerated stability test by continuously applying linear potential sweeps from 0.6 to 1.1 V, which caused surface oxidation/reduction cycles of Pt. The surface reaction involves the formation of PtOH and PtO derived from the oxidation of water that causes the dissolution of Pt via the $Pt^{2+}$ oxidation state (*12*). We conducted the test by applying potential sweeps at the rate of 50 mV/s to a thin-layer rotating disk electrode in an $O_2$-saturated 0.1 M $HClO_4$ solution at room temperature. For comparison, a Pt/C catalyst with the same Pt loading as that in Au/Pt/C was subjected to the same potential cycling conditions. After 30,000 cycles, changes in the Pt surface area and electrocatalytic activity of the ORR were determined.

The catalytic activity of Au/Pt/C, measured as the currents of $O_2$ reduction obtained before and after potential cycling, showed only a 5-mV degradation in half-wave potential over the cycling period (Fig. 3A); in contrast, the corresponding change for Pt/C amounts to a loss of 39 mV (Fig. 3C). The same experiment with Au/Pt/C at 60°C showed no loss of activity (fig. S5), affording additional evidence for the stabilizing effect of Au clusters on the underlying Pt.

Voltammetry was used to determine the Pt surface area of the Au/Pt/C and Pt/C electrodes by measuring H adsorption before and after potential cycling. Integrating the charge between 0 and 0.36 V associated with H adsorption for Au/Pt/C shows no change, indicating no recordable loss of Pt surface area (Fig. 3B). However, for Pt/C, only ~55% of the original Pt surface area remained after potential cycling (Fig. 3D). As expected, the surface-area measurements are in good agreement with the measured ORR activities.

For the Pt/C catalyst (11.9 $\mu g_{Pt}/cm^2$), the measured degradation of the half-wave potential ($E_{1/2}$) after 30,000 cycles (at room temperature) was 39 mV. If the Pt specific activity does not vary significantly with the potential cycling, and assuming a constant Tafel slope $b$ of –120 mV, the remaining Pt surface area after potential cycling can be estimated by using the expression (see the supporting online material) $\Delta E_{1/2} = -b \times \log(S_{Pt}/S_{Pt0})$, where $S_{Pt}$ is the Pt surface area after cycling and $S_{Pt0}$ is the initial Pt surface area. For the loss in $E_{1/2}$ of 39 mV, the calculated value for the remaining active Pt surface area is 47% of the initial one. This is less than the observed 55%, but the difference is not surprising given a possible change of the interfacial conditions during

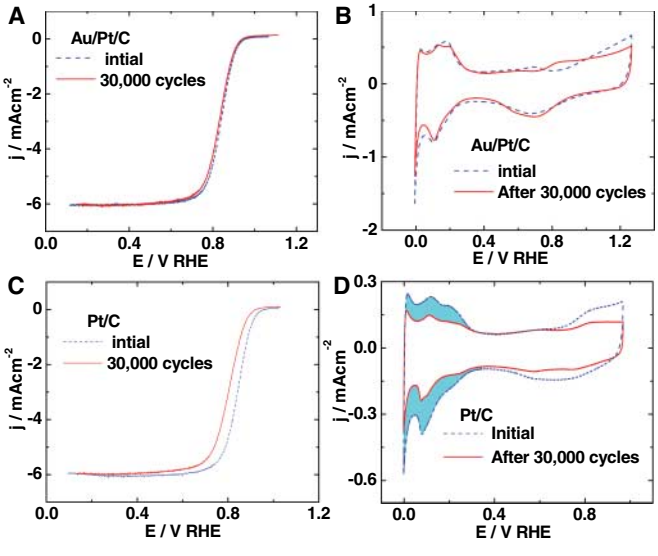


**Fig. 3.** Polarization curves for the $O_2$ reduction reaction on Au/Pt/C (**A**) and Pt/C (**C**) catalysts on a rotating disk electrode, before and after 30,000 potential cycles. Sweep rate, 10 mV/s; rotation rate, 1600 rpm. Voltammetry curves for Au/Pt/C (**B**) and Pt/C (**D**) catalysts before and after 30,000 cycles; sweep rate, 50 and 20 mV/s, respectively. The potential cycles were from 0.6 to 1.1 V in an $O_2$-saturated 0.1 M $HClO_4$ solution at room temperature. For all electrodes, the Pt loading was 1.95 μg (or 10 nmol) of Pt on a 0.164 $cm^2$ glassy carbon rotating-disk electrode. The shaded area in (D) indicates the lost Pt area.

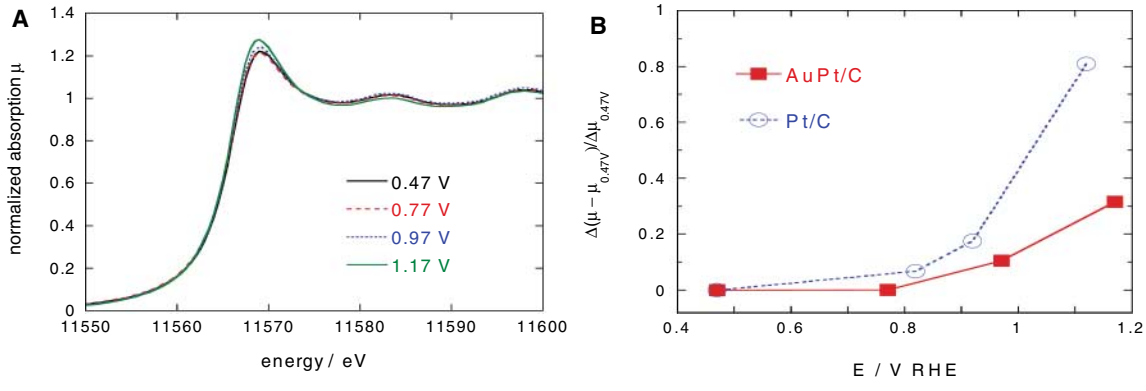


**Fig. 4.** (**A**) XANES spectra obtained with the Au/Pt/C catalyst at the Pt $L_3$ edge at four different potentials. (**B**) A comparison of the change of the absorption edge peaks of the XANES spectra for Au/Pt/C and Pt/C as a function of potential, obtained with the electrocatalysts at four different potentials in 1 M $HClO_4$.

30,000 cycles and the approximations involved in the calculation. A similar expression for the cell can be found in reference (*11*).

This stabilizing effect of Au clusters and lack of ORR inhibition, despite blockage of approximately one-third of the Pt sites on Au/Pt/C by Au, are intriguing phenomena that may have additional applications beyond fuel cells. To elucidate the origin of the observed stabilization effect of Au clusters, we determined by in situ x-ray absorption near edge spectroscopy (XANES) the oxidation state of Pt as a function of potential for the Au/Pt/C and Pt/C surfaces. The data offer strong evidence of decreased oxidation of Pt nanoparticles covered by Au in comparison with the oxidation of Pt nanoparticles lacking such coverage. In the XANES spectra for Au/Pt/C at the Pt $L_3$ edge (Fig. 4A), the intensity of the absorption bands reflects the depletion of the *d* band caused by the oxidation of Pt; a very small potential dependence indicates such oxidation. This effect is more evident in the relative change of the x-ray absorption peak intensity of the Pt $L_3$ edge spectra for Au/Pt/C and Pt/C as a function of potential (Fig. 4B). The increase in the intensity of the absorption edge peak for the Au/Pt/C electrocatalyst commences at considerably higher potentials than does that for the Pt/C catalyst; thus, the oxidation of Pt nanoparticles modified by Au clusters requires much higher potentials than are necessary for unmodified Pt nanoparticles. The high Pt oxidation potential of the Au/Pt/C electrocatalyst (that is, the lower extent of Pt oxidation) is clearly the major mechanism for the stabilization effect of Au clusters. A decreased Pt oxidation can also be discerned from a comparison of voltammetry curves for Au/Pt/C and Pt/C, as well as for Au/Pt(111) and Pt(111). The lower charge associated with the Pt oxidation at the potential region between 0.7 and 1.1 V clearly reveals the reduced oxidation of Au-modified surfaces (fig. S6). Table 1 gives a summary of the observed changes in surface area and catalytic activity data caused by potential cycling.

Nørskov and co-workers recently proposed a model describing the activity of metal adlayers (*14*, *15*), according to which the characteristics of the surface metal *d* bands, particularly the weighted center ($\varepsilon_d$), play a decisive role in determining surface reactivity. Density functional theory (DFT) calculations showed that the binding energies and reactivity of small adsorbates correlate well with the position of $\varepsilon_d$ on strained surfaces and metal overlayers (*16*), in accordance with data from numerous experimental studies (*17*–*20*). The small Au clusters have more low-coordinate Au atoms than do the extended Au crystal surfaces. Au atoms with low coordination numbers have higher-lying *d* states, which are more reactive and interact more strongly with the adsorbate states (*21*). Au clusters on oxide supports can thereby activate molecular oxygen at room temperature (*22*–*24*).

When Au clusters are bound on a metallic, rather than oxide, substrate, the electronic interactions differ. Roudgar and Groβ (*25*) used DFT calculations to demonstrate a significant coupling of *d* orbitals of small Pd clusters to the Au(111) substrate. An equivalent type of interaction between Au and Pt can account for the observed stabilization of Pt. When clusters of the softer Au metal are placed on the surface of considerably harder Pt, there is practically no mixing between them. Del Pópolo *et al*. (*26*) previously reached a similar conclusion regarding Pd on an Au system. The surface alloying of Au with Pt, although unlikely, also would modify the Pt electronic structure toward a lower Pt surface energy, or lower-lying Pt *d*-band states.

The high ORR activity of the Au clusters on a modified Pt/C electrocatalyst is a counterintuitive observation. Au is not an active catalyst for the ORR to $H_2O$; instead, $H_2O_2$ is quantitatively generated in a two-electron reduction at most surfaces [except for Au(100) and its vicinal surfaces in alkaline solutions (*27*)]. Because Pt reduces $O_2$ to $H_2O$ in a four-electron process, a decrease of the reduction current for the Pt surface that is one-third covered by a monolayer of Au would be expected. Without this decrease, it appears that Au clusters have a very high activity, in stark contrast to the behavior of the bulk Au or of carbon-supported Au nanoparticles. As discussed above, the mechanism of oxygen activation by Au clusters is controversial. Several researchers ascribed the activity of Au clusters to their interactions with oxides, resulting in charged Au particles (*28*). In view of our preceding discussion (*25*), such a process is not likely to occur with Au clusters at metal supports. To explain the observed activity, we might consider an efficient spillover of $H_2O_2$ from Au clusters to the surrounding Pt atoms, where further reduction to $H_2O$ can take place. Alternatively, if AuOH is formed at certain potentials, it may help in reducing $H_2O_2$, as discussed for alkaline solutions (*29*). Such behavior could account for the negligible loss of activity of the Pt surface toward ORR.

Our studies raise promising possibilities for synthesizing improved ORR Pt-based catalysts and for stabilizing Pt and other Pt-group metals under oxidizing conditions.

**Table 1.** A comparison of surface area and the catalytic activity data for Pt/C and Au/Pt/C before and after 30,000 potential cycles from 0.6 to 1.1 V under the oxidizing conditions of the $O_2$ reduction reaction. Data were obtained from Fig. 3.

| Catalyst and kinetic data | Pt dispersion ($m^2/g_{Pt}$) | Half-wave potential at 1600 rpm (V) | Kinetic current density at 0.85 V ($mA/cm^2$) | Specific kinetic current density at 0.85 V ($A/m^2_{Pt}$) |
|---|---|---|---|---|
| Pt/C initial | 65.5 | 0.841 | 4.56 | 5.80 |
| Pt/C after 30,000 cycles | 35.5 | 0.802 | 1.60 | 3.72 |
| Au/Pt/C initial | 63.1 | 0.838 | 4.23 | 5.64 |
| Au/Pt/C after 30,000 cycles | 60.6 | 0.833 | 4.10 | 5.69 |

## References and Notes


1. Y. Iizuka *et al.*, *Catal. Today* **36**, 115 (1997).
2. M. Comotti, W. C. Li, B. Spliethoff, F. Schuth, *J. Am. Chem. Soc.* **128**, 917 (2006).
3. M. Valden, X. Lai, D. W. Goodman, *Science* **281**, 1647 (1998).
4. C. C. Chusuei, X. Lai, K. Luo, D. W. Goodman, *Top. Catal.* **14**, 71 (2001).
5. D. C. Meier, D. W. Goodman, *J. Am. Chem. Soc.* **126**, 1892 (2004).
6. R. Meyer, C. Lemire, S. K. Shaikhutdinov, H. Freund, *Gold Bull.* **37**, 72 (2004).
7. M. S. Chen, D. W. Goodman, *Catal. Today* **111**, 22 (2006).
8. B. Hammer, *Top. Catal.* **37**, 3 (2006).
9. B. K. Min, W. T. Wallace, D. W. Goodman, *Surf. Sci.* **600**, L7 (2006).
10. H. A. Gasteiger, S. S. Kocha, B. Sompalli, F. T. Wagner, *Appl. Catal. B Environ.* **56**, 9 (2005).
11. P. J. Ferreira *et al.*, *J. Electrochem. Soc.* **152**, A2256 (2005).
12. R. Woods, in *Electroanalytical Chemistry*, A. J. Bard, Ed. (Marcel Dekker, New York, 1976), vol. 9.
13. S. R. Brankovic, J. X. Wang, R. R. Adzic, *J. Serb. Chem. Soc.* **66**, 887 (2001).
14. J. Greeley, J. K. Nørskov, M. Mavrikakis, *Annu. Rev. Phys. Chem.* **53**, 319 (2002).
15. B. Hammer, J. K. Nørskov, in *Advances in Catalysis* (Elsevier, Amsterdam, 2000), vol. 45, pp. 71–129.
16. Y. Xu, A. V. Ruban, M. Mavrikakis, *J. Am. Chem. Soc.* **126**, 4717 (2004).
17. E. Christoffersen, P. Liu, A. Ruban, H. L. Skriver, J. K. Nørskov, *J. Catal.* **199**, 123 (2001).
18. F. B. de Mongeot, M. Scherer, B. Gleich, E. Kopatzki, R. J. Behm, *Surf. Sci.* **411**, 249 (1998).
19. J. A. Rodriguez, D. W. Goodman, *Science* **257**, 897 (1992).
20. J. Zhang, M. B. Vukmirovic, Y. Xu, M. Mavrikakis, R. R. Adzic, *Angew. Chem. Int. Ed.* **44**, 2132 (2005).
21. N. Lopez, J. K. Nørskov, *J. Am. Chem. Soc.* **124**, 11262 (2002).
22. Y. D. Kim, M. Fischer, G. Gantefor, *Chem. Phys. Lett.* **377**, 170 (2003).
23. D. Stolcic *et al.*, *J. Am. Chem. Soc.* **125**, 2848 (2003).
24. B. E. Salisbury, W. T. Wallace, R. L. Whetten, *Chem. Phys.* **262**, 131 (2000).
25. A. Roudgar, A. Groß, *Surf. Sci.* **559**, L180 (2004).
26. M. G. Del Pópolo, E. P. M. Leiva, M. Mariscal, W. Schmickler, *Surf. Sci.* **597**, 133 (2005).
27. R. Adzic, in *Electrocatalysis*, J. Lipkowski, P. N. Ross, Eds. (Wiley-VCH, New York, 1998), pp. 197–242.
28. B. Yoon, H. Hakkinen, U. Landman, *J. Phys. Chem. A* **107**, 4066 (2003).
29. S. Strbac, R. R. Adzic, *J. Electroanal. Chem.* **403**, 169 (1996).


30. This work is supported by the U.S. Department of Energy, Divisions of Chemical and Material Sciences, under contract no. DE-AC02- 98CH10886. We thank H. Isaacs for helpful discussions.


## Supporting Online Material

www.sciencemag.org/cgi/content/full/315/5809/220/DC1
SOM Text
Figs. S1 to S6

31 August 2006; accepted 15 November 2006
10.1126/science.1134569